# Selective oxidation of propane on MgO/$\gamma$-$Al_2O_3$-supported molybdenum catalyst: influence of promoters

M.C. Abello *, M.F. Gomez and L.E. Cadus

*INTEQUI, Instituto de Investigaciones en Tecnología Química (UNSL-CONICET), Casilla de Correo 290, 5700 San Luis, Argentina*
E-mail: intequi@unsl.edu.ar

Received 12 November 1997; accepted 7 May 1998

The influence of promoters, potassium and samarium, on molybdenum supported over MgO–$\gamma$-$Al_2O_3$ catalyst has been investigated in the oxidative dehydrogenation of propane. The acidities of catalysts were determined by temperature-programmed desorption of $NH_3$ and by decomposition of 2-propanol. The K-promoted catalyst showed the lower acidity followed by the Sm, whereas the unpromoted sample showed the highest acidity. The higher the acid character of the catalyst, the lower the selectivity to propene. Redox properties determined from EPR spectra change with the addition of the promoter. A parallelism between $Mo^{6+}$ reducibility and catalytic activity was found.

**Keywords:** oxidehydrogenation of light paraffins, propane oxidation, redox and acid–base properties, promoters, molybdenum catalyst

## 1. Introduction

The selective oxidation of light alkanes to produce alkenes or oxygenated compounds is receiving great attention due to its potential application as a source of cheap raw materials. A wide variety of catalytic systems has been proposed for this reaction, VMgO being the most promisory one [1–6]. Recently, the MgMoO system has been reported to be active and relatively selective in the oxidehydrogenation (ODH) of propane to propene [7–11]. Conversions of propane between 2.6 and 32% and selectivities to propene between 86 and 27%, respectively, were found on molybdenum supported over MgO–$\gamma$-$Al_2O_3$ [9]. The dehydrogenation selectivity was reduced by the formation of carbon oxides. The partial oxidation of organic compounds usually implies a Mars and van Krevelen mechanism involving cations of which the oxidation states vary during the catalytic cycle and lattice oxygen ions which could be inserted in the substrate molecule or they can facilitate its dehydrogenation by forming $H_2O$ [12]. The acid–base and redox properties of catalysts are obviously of prime importance. Considerable efforts are made to relate these properties with activity or selectivity [12–14]. It is well known that some promoters modify not only the redox properties of the system but also the acid–base character of the oxygen species present on the catalyst surface. Valenzuela et al. [15] have studied the effect of different additives on the performance of VMgO catalyst in the oxidative dehydrogenation of propane. They assumed that the easier the reducibility of V ions, the higher the selectivity to propene. Galli et al. [14] suggested that the addition of potassium on alumina-supported vanadia decreased both the reducibility of V and the number of surface acid sites, thus increasing the selectivity to $C_4$-olefins from butane and decreasing the selectivity to ethene from ethane. The additions of other alkali metal and rare earths have also been studied [16,17].

In the present work, the influence of potassium and samarium on redox and acid–base properties of MgO–$\gamma$-$Al_2O_3$-supported molybdenum has been investigated in order to develop a more efficient catalyst for the oxidative dehydrogenation of propane.

## 2. Experimental

### 2.1. Catalyst preparation

Mo supported on MgO–$\gamma$-$Al_2O_3$ was prepared by using the impregnation procedure described elsewhere [9]. The composite support (16% of magnesium on alumina, 16S, specific surface area 140 $m^2$/g), was impregnated with a solution of ammonium heptamolybdate and calcined at 873 K for 5 h to form the original catalyst named Mo16S. Promoted samples, containing 2 wt% of K and Sm, were prepared by adding the required amount of the respective compound ($KNO_3$ in aqueous solution or $Sm_2O_3$ in citric acid solution) through the wet impregnation method. Then, they were dried and calcined at 873 K. The catalysts were denoted further in the text by XMo16S, where X = K or Sm.

### 2.2. Catalyst characterization

Specific surface areas ($S_{BET}$, $m^2$/g) of all samples were determined from nitrogen adsorption isotherms at 77 K by the BET method. A Micromeritics Accusorb 2100E apparatus was used.

---

* To whom correspondence should be addressed.

X-ray diffraction (XRD) patterns were obtained by using a Rigaku diffractometer operated at 30 kV and 20 mA by employing Ni-filtered Cu K$\alpha$ radiation ($\lambda = 0.15418$ nm).

The EPR measurements were obtained with a Bruker spectrometer at room temperature and a Klystron frequency of 9.7 GHz and 100 kHz magnetic field modulation.

Temperature-programmed reduction (TPR) studies were performed in a TPR conventional unit. This apparatus consists of a gas handling system with mass flow controllers (Mathesson), a tubular reactor, a linear temperature programmer (Omega, model CN 2010), a PC for data retrieval, a furnace and various cold traps. Samples of ca. 100 mg were first oxidized in a 30 ml/min flow of 20 vol% $O_2$ in He at 873 K for 30 min and then cooled at room temperature. After that, helium was admitted at room temperature to remove oxygen. The samples were subsequently contacted with a 30 ml/min flow of 5 vol% $H_2$ in $N_2$ and heated at a rate of 10 K/min to a final temperature of 1000 K, while hydrogen consumption was monitored by a thermal conductivity detector after removing the water formed. Hydrogen consumption was determined by means of the response calibration, performed before and after each TPR.

Acidity measurements were determined by ammonia temperature-programmed desorption, TPD, by using a conventional flow system with a thermal conductivity detector. The adsorption step was carried out in pure ammonia flow for 30 min at room temperature. Then, the samples were swept with helium for 30 min and, finally, the desorption step was performed from room temperature to 823 K at a heating rate of 10 K/min. Continuous voltages from the detector cell and reactor thermocouple were converted to digital signals, amplified with a data acquisition workstation and stored in a PC. An arbitrary scale for the different acid strengths was selected. Weak, medium and strong acidity were related to the number of $NH_3$ molecules desorbed up to 473 K, between 473 and 673 K and above 673 K, respectively. The acidity distribution of catalysts has been expressed as the ratio between the integrated area of the $NH_3$ band developed in a given range of temperature and the total integrated area of the $NH_3$ band. Acidity was calculated by dividing the total area by the BET surface area of the sample.

Decomposition of isopropanol, IPA, was used for determining the acid–base properties of the samples [18]. Since IPA needs an acid–base pair to be converted to acetone, the acetone-to-propene ratio reflects the basicity, whereas the propene formation rate is due to the acidity. The reaction was carried out at 453 K in a fixed-bed continuous-flow reactor under atmospheric pressure. The feed consisted of 4.5% IPA and the balance was helium. The flow rate was 40 ml(STP) $\text{min}^{-1}$, and the conversion of 2-propanol was $<15\%$ in all experiments. Product analysis was performed by gas chromatography using a Carbowax 20 M on Chromosorb W column and a thermal conductivity detector.

### 2.3. Catalytic test

The catalysts (0.5–0.85 mm particles diameter) were tested in a fixed-bed, quartz tubular reactor operated at atmospheric pressure between 723 and 823 K. The temperature was measured with a coaxial thermocouple. The feed was a mixture of 4 vol% propane, 4 vol% oxygen and the balance helium. The flow rate was 100 ml/min at room temperature. The reactants and reaction products were alternately analyzed on-line by a Shimadzu GC9A gas chromatograph equipped with a thermal conductivity detector. A Porapaq Q (80–100 mesh) column for separating hydrocarbons and $CO_2$ and a 2 m Activated Carbon (30–50 mesh) column for carbon monoxide, methane and oxygen were used. The catalyst weight was varied between 0.5 and 1 g. Different contact times, $W/F$ in $g_{\text{cat}}\,h\,(\text{mol}\ C_3H_8)^{-1}$, were used to obtain different propane conversion levels. The homogeneous contribution was tested with the empty reactor. These runs showed no activity below 853 K. The results were very similar with and without the use of quartz particles.The conversion and selectivity for products were evaluated for the exit stream. Heat and mass transfer limitations were not observed under the experimental conditions used.

## 3. Results

### 3.1. Catalyst characterization

The specific surface areas of the samples are shown in table 1. The BET values of promoted catalysts were slightly higher than the original one. The BET area of Mo16S agrees with the value given in [9], indicating that the reproducibility of the preparation procedure was highly satisfactory. The addition of K increased slightly the BET area (around 10%), while the increase for the Sm-doped sample was 22%. Similar results have been found in literature [15].

The X-ray diffraction patterns of unpromoted and promoted catalysts only showed the presence of $MgMoO_4$, characterized by the principal line at $2\theta = 26.4$ ($d = 3.37$) and $\gamma$-$Al_2O_3$ [9]. There was no identification of the presence of another phase or structure, probably because of their low concentration in the solid. After being used in propane oxidation, no remarkable changes were observed in the XRD patterns.

TPR profiles of the catalysts are presented in figure 1. The results showed that all samples had only one broad reduction peak with a maximum, practically at the same temperature range. Since $Al_2O_3$ does not undergo reduction by hydrogen at these temperatures, the peak can be attributed to the reduction of molybdenum ions. In fact,

Table 1
Specific surface areas of unpromoted and promoted molybdenum catalysts.

| Sample | Mo16S | KMo16S | SmMo16S |
|---|---|---|---|
| $S_{\text{BET}}$ ($m^2$/g) | 59.7 | 67.3 | 72.8 |

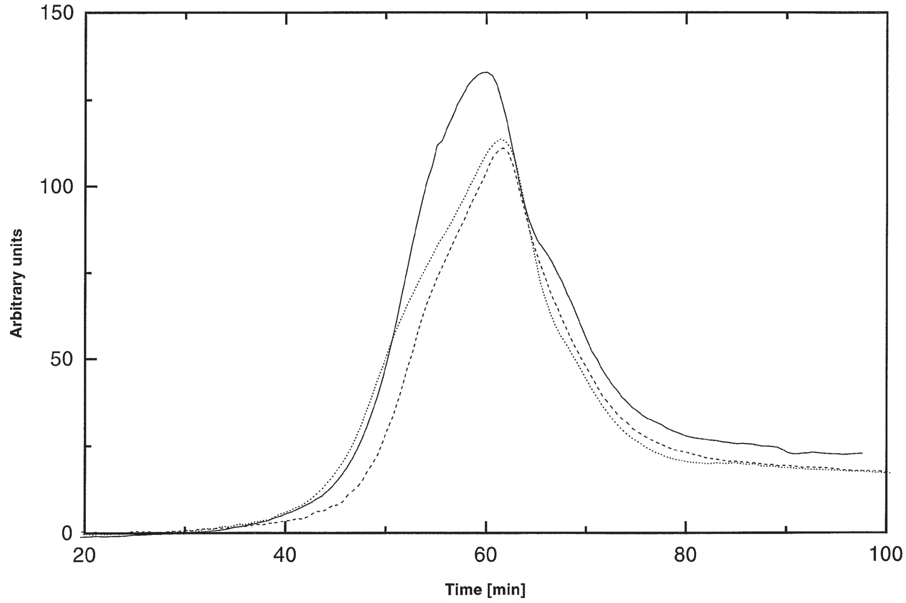

Figure 1. TPR profiles of molybdenum supported MgO/$\gamma$-$Al_2O_3$ catalysts. (—) SmMo16S; (····) Mo16S, (· · ·) KMo16S.

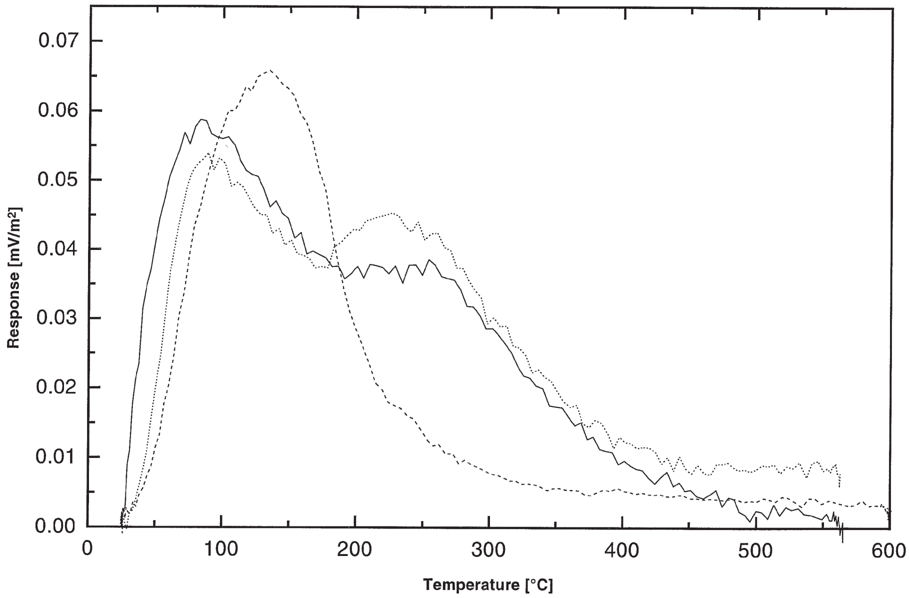

Figure 2. $NH_3$-TPD profiles of molybdenum supported MgO/$\gamma$-$Al_2O_3$ catalysts. (—) SmMo16S; (····) Mo16S, (· · ·) KMo16S.

the XRD patterns of the Mo16S used in the TPR experiment revealed the presence of $MoO_2$. MgO and $MgMoO_4$ were not detected. The reduction started around 573 K and the $H_2$ consumption per Mo atom corresponded to about 90% of the total $Mo^{6+}$ to $Mo^{4+}$ reduction. The onset temperature, $T_O$, the temperature of the maximum hydrogen consumption, $T_M$, and the $H_2$ consumption calculated from the TPR areas for all samples are listed in table 2.

$NH_3$-TPD patterns for the samples between 298 and 853 K are shown in figure 2. Mo16S and SmMo16S show similar profiles, whereas a narrower peak is observed on KMo16S. Acid strength distribution, calculated as explained in section 2, is illustrated in figure 3. The specific acidity (total acidity per $m^2$) decreased in the following order: Mo16S $\approx$ SmMo16S $>$ KMo16S. The three samples showed a low abundance of strong sites (6.8% for Mo16S, 3.9% for SmMo16 and 4.3% for KMo16S, respectively). The unpromoted catalyst showed a similar amount of medium (49.4%) and weak (43.8%) acid sites,

Table 2
Temperature-programmed reduction of MgO/$Al_2O_3$-supported molybdenum catalysts.

| Sample | $H_2$ consumption (mmol/g) | $T_O$ (K) | $T_M$ (K) |
|---|---|---|---|
| Mo16S | 3.1 | 573 | 912 |
| KMo16S | 3.0 | 573 | 915 |
| SmMo16S | 3.7 | 573 | 899 |

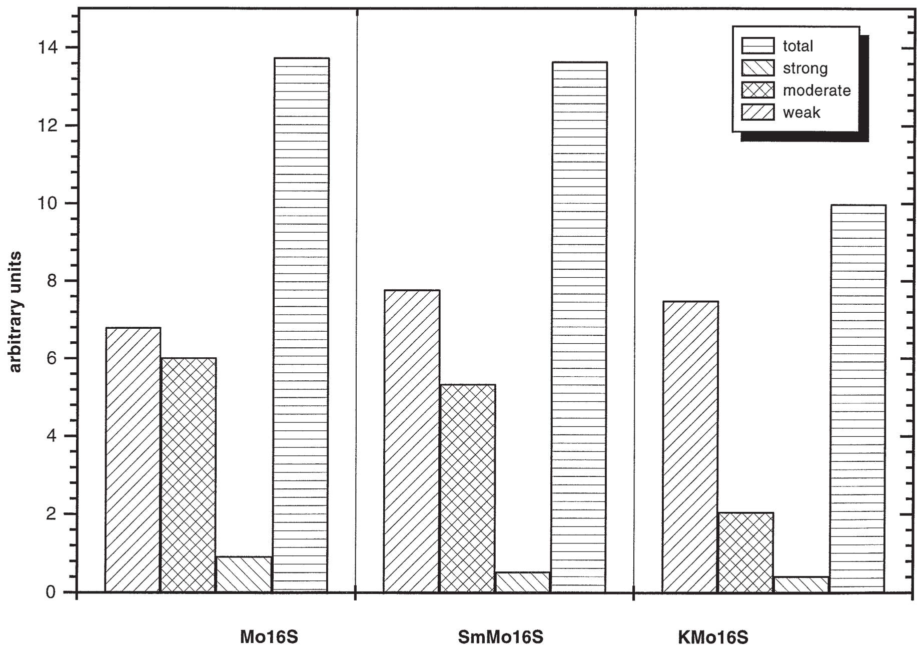

Figure 3. Acidity distribution from $NH_3$-TPD measurements.

Table 3
Basicity (acetone-to-propene ratio) and acidity (propene formation rate) of unpromoted and promoted catalysts determined by decomposition of 2-propanol.

| Catalyst | $r(\mathrm{P}) \times 10^9$ ($\mathrm{mol\,m^{-2}\,s^{-1}}$) | $r(\mathrm{A}) \times 10^{10}$ ($\mathrm{mol\,m^{-2}\,s^{-1}}$) | Basicity ($r(\mathrm{A})/r(\mathrm{P})$) |
|---|---|---|---|
| Mo16S | 6.1 | 4.5 | 0.07 |
| SmMo16S | 5.0 | 4.6 | 0.09 |
| KMo16S | 0.76 | 3.2 | 1.15 |

whereas SmMo16S showed a slight increase in weak acidity (56.7%). However, the 75% of the whole acidity on KMo16S corresponded to weak acid sites markedly decreasing the moderate acidity (20.7%). The $NH_3$-TPD pattern of the bare support was also obtained. The addition of Mg to alumina slightly affects the stronger acid sites and promotes an increase in the weaker acidity [19].

The samples were also characterized by isopropanol decomposition, a probe reaction for the acid–base properties of the catalysts. Alcohol decomposes through two parallel routes: dehydration to propene on a Brønsted $H^+$ site or on a Lewis acid–base pair and dehydrogenation to acetone, a reaction in which the acid–base pair is involved [18]. The formation rates of propene and acetone are shown in table 3. In all samples the dehydration to propene was the predomimant reaction, which indicates that catalysts are acid. The addition of promoters decreased the propene formation rate, KMo16S being the more affected one. Acetone formation rate was nearly constant in all samples. The highest surface basicity (the acetone-to-propene ratio) was observed for KMo16S. These results agree with acidity values given by $NH_3$-TPD.

EPR spectroscopy was used to examine the presence of $Mo^{5+}$ and to evaluate changes in the signal intensity of promoted catalysts. The measurements were carried out on fresh samples and in those used in the oxidehydrogenation of propane. The spectra of both fresh and used samples were well resolved and exhibited an asymmetric EPR signal with an average $g$ value of 1.928, which was assigned to $Mo^{5+}$ in an environment of nonaxial symmetry [9]. This value was very close to those values reported by other workers [20,21]. The $g$ values and line width at peak-to-peak maximum ($\Delta H_{\mathrm{pp}}$) are presented in table 4. Figure 4 shows the EPR spectra for samples before and after oxidative dehydrogenation of propane. The intensities of the signal were different, and a comparison can be made on the basis of a similar $\Delta H_{\mathrm{pp}}$ value. The intensities of the lines for used samples were remarkably more intense than for fresh samples. The intensity decreased in the order of Mo16S $>$ SmMo16S $>$ KMo16S, as is evident from table 4. KMo16S hardly shows the EPR signal in the fresh sample.

### 3.2. Catalytic test

The catalytic results, obtained in the oxidative dehydrogenation of propane on Mo supported over MgO–$\gamma$-$Al_2O_3$ and on its samples modified with 2 wt% of different promoters, are shown in table 5. Propene, CO and $CO_2$ were the main products. Small amounts of $C_2H_6$ and $C_2H_4$ were also detected. Other oxygenated products were not observed. Figure 5 shows the variation of the conversion of propane with contact time, $W/F$ at 773 and 823 K. Conversion nearly follows a linear relationship with respect to contact time. Then, the oxidation of propane occurs mainly on the surface, and product formation does not inhibit the reaction. The catalytic activity decreases in the order Mo16S $>$ SmMo16S $>$ KMo16S. At the lowest reaction temperature, 723 K, the activities of both promoted

Table 4
EPR parameters of the signals for Mo supported catalysts.

| Catalyst | Av. $g$ | | $\Delta H_{pp}$ | Intensity $I$ (g sample) | | $\Delta I$ |
|---|---|---|---|---|---|---|
| | b.r. | a.r. | Gauss | b.r. | a.r. | |
| Mo16S | 1.9280 | 1.9280 | 57 | 17.9 | 234.1 | ×13 |
| SmMo16S | 1.9285 | 1.9288 | 58 | 10.5 | 94.4 | ×9 |
| KMo16S | 1.9282 | 1.9277 | 59 | 4.5 | 13.8 | ×3 |

b.r.: before reaction; a.r.: after reaction.

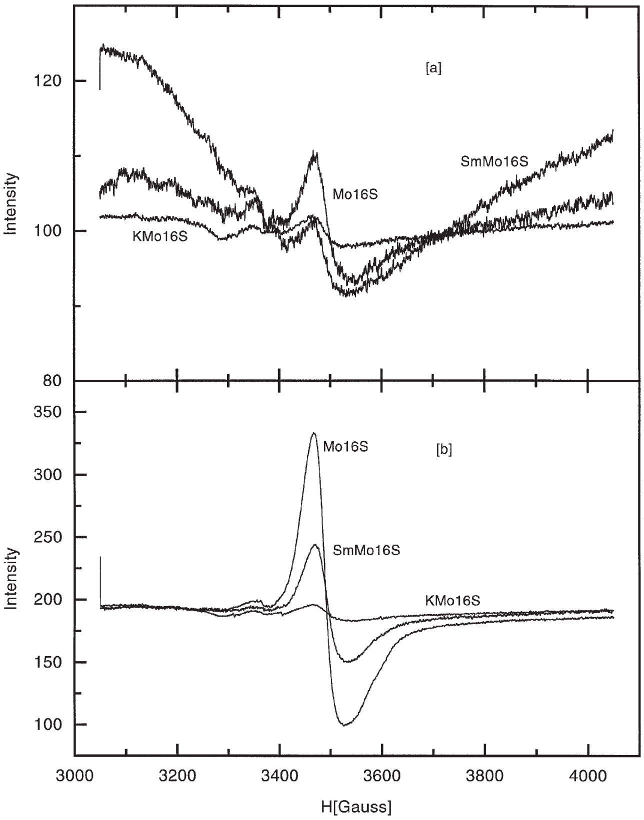

Figure 4. EPR spectra of fresh (a) and used samples (b).

catalysts were similar, but they remained being lower than the activity of the original one.

The variation of selectivity to propene as a function of conversion is shown in figure 6. The selectivity decreased with increasing propane conversion in all samples. It appears to be little dependent on temperature in the studied temperature range and much more dependent on the extent of propane conversion. The selectivity to propene decreased more rapidly on Mo16S than on doped samples. It can be seen that the selectivity to propene on KMo16S is higher than on SmMo16S and Mo16S. Some of these results are also summarized in table 6, in which the selectivities to propene at the same conversion level are compared. The decrease in propene selectivity is accompanied by a considerable increase in the selectivity to carbon monoxide, whereas the selectivity to carbon dioxide changes more smoothly. The selectivity to CO and to a less extent to $CO_2$ increases with reaction temperature. The $CO/CO_2$ ratio reaches a value which is almost constant (about 2.5). The CO selectivity becomes null at low conversion, while $CO_2$ always shows a selectivity greater than 4%. This behavior and the high $CO/CO_2$ ratio can suggest that CO is fundamentally a secondary product and $CO_2$ can also be formed directly from propane.

## 4. Discussion

From the results it is clear that the promoters investigated in this work greatly influence the catalytic performance of Mo supported on MgO–$\gamma$-$Al_2O_3$ in the ODH of propane. The modifications observed in the redox and acid–base properties of the promoted catalysts can explain the different behavior found.

The addition of Sm does not change the whole acidity, but promotes a slight redistribution of acid sites. An increase of around 15% in the weak acidity (up to 473 K) is found at the expense of moderate and strong acidity. On the other hand, the addition of K markedly decreases moderate acidity and correspondingly increases weak acidity. It is likely that the ratio between Brønsted and Lewis acid sites concentration changes due to the formation of weak surface acid sites (associated to alkali metal cations) and the cancellation of Brønsted sites due to alkali molybdate formation. No XRD line could be unequivocally assigned to $K_2MoO_4$. However, Martin et al. [22] could assign XRD lines to molybdenum oxocompounds on 1% K-doped $MoO_3/TiO_2$ sample, and they found a mixture of crystalline $K_2Mo_2O_7$ and $K_2MoO_4$ on 3% K. The presence of a slight excess of $MoO_3$ over the $MgMoO_4$ particles on Mo16S has been reported [9]. Then, the formation of alkali molybdate could be possible. The strong acid sites present on Mo16S are converted into weak acid sites by the addition of both dopants.

An increase in the relative surface basicity in the order of KMo16S $>$ SmMo16S $>$ Mo16S is also revealed by decomposition of isopropanol (table 3). The main product in the IPA reaction was propene in all the samples, indicating that the surface has mainly acidic properties. Mo16S and SmMo16S are comparably active for both dehydrogenation and dehydration. SmMo16S shows only small changes in isopropanol dehydration/dehydrogenation ratio, whereas a drastic change occurs with the addition of K. The latter affects dehydration activity to a greater extent, which is probably related to the moderate and strong acidity in agreement with $NH_3$-TPD. Since acetone formation rates are nearly the same in all catalysts, it seems that the

Table 5
Oxidative dehydrogenation of propane on supported molybdenum catalysts.

| Sample | $W/F$ | $T$ | Conversion | Selectivity (%) | | | |
|---|---|---|---|---|---|---|---|
| | (g h mol$^{-1}$) | (K) | (%) | $\mathrm{C}_3^{=}$ | CO | $\mathrm{CO}_2$ | $\mathrm{C}_2$ |
| Mo16S | 54.9 | 723 | 2.3 | 78.7 | – | 21.3 | – |
| | | 773 | 9.6 | 42.5 | 40.6 | 15.7 | 1.2 |
| | | 823 | 19.6 | 34.4 | 44.6 | 19.2 | 1.8 |
| | 77.0 | 723 | 2.9 | 88.6 | – | 11.4 | – |
| | | 773 | 13.0 | 52.5 | 35.0 | 12.5 | – |
| | | 823 | 27.9 | 35.7 | 45.3 | 17.4 | 1.5 |
| | 109.9 | 723 | 9.0 | 44.4 | 39.9 | 15.6 | – |
| | | 773 | 18.9 | 41.6 | 41.2 | 16.0 | 1.1 |
| | | 823 | 34.8 | 30.2 | 46.5 | 21.2 | 2.1 |
| KMo16S | 55.0 | 723 | 2.0 | 95.5 | – | 4.5 | – |
| | | 773 | 5.0 | 92.4 | – | 7.6 | – |
| | | 823 | 13.8 | 62.6 | 26.3 | 11.0 | – |
| | 76.9 | 723 | 2.7 | 94.0 | – | 6.0 | – |
| | | 773 | 6.5 | 90.0 | – | 9.9 | – |
| | | 823 | 18.6 | 52.2 | 34.9 | 12.9 | – |
| | 110.4 | 723 | 3.9 | 90.2 | – | 9.8 | – |
| | | 773 | 11.8 | 62.4 | 26.4 | 11.2 | – |
| | | 823 | 26.4 | 44.7 | 38.1 | 16.0 | 1.1 |
| SmMo16S | 54.9 | 723 | 2.6 | 92.2 | – | 7.7 | – |
| | | 773 | 6.7 | 78.7 | 7.1 | 14.2 | – |
| | | 823 | 19.7 | 45.2 | 38.7 | 14.7 | 1.3 |
| | 76.9 | 723 | 3.2 | 88.8 | – | 11.2 | – |
| | | 773 | 10.5 | 62.7 | 22.4 | 14.9 | – |
| | | 823 | 25.2 | 40.3 | 41.2 | 17.2 | 1.3 |
| | 109.9 | 723 | 4.7 | 84.5 | – | 15.5 | – |
| | | 773 | 17.2 | 45.6 | 39.1 | 15.2 | – |
| | | 823 | 32.9 | 29.3 | 47.7 | 21.1 | 1.9 |

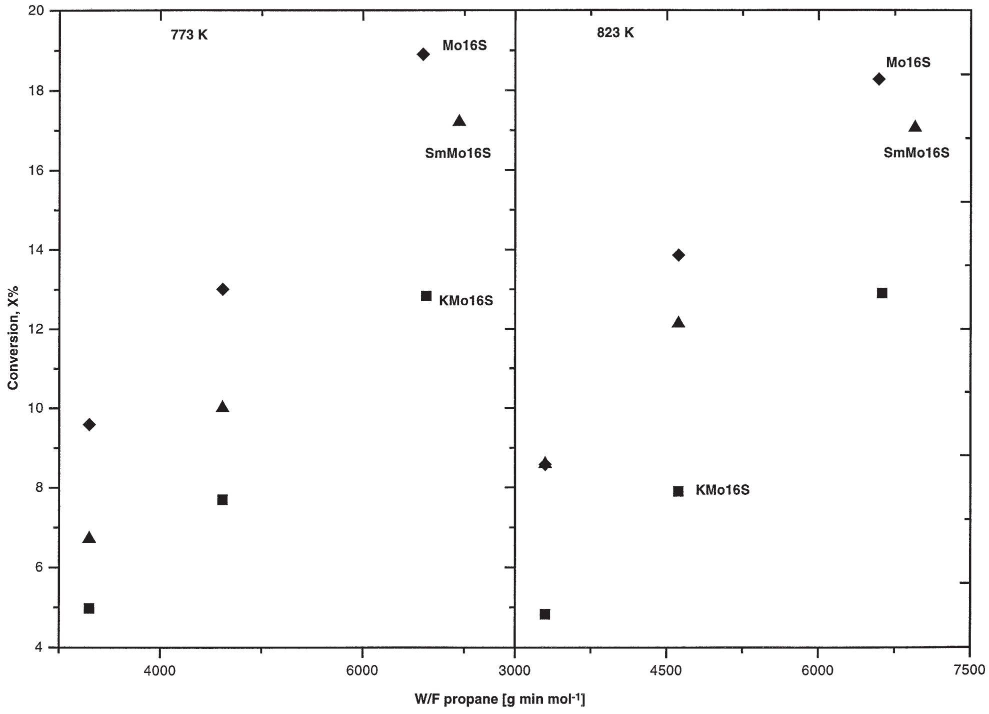

Figure 5. Variation of the conversion of propane with the contact time, $W/F$.

acid–base pair concentration, involved in dehydrogenation reaction, is not significantly affected by the addition of promoters. Gervasini and Auroux [18] have also suggested that the dehydrogenation of isopropanol to acetone is not influenced by the strength of either the acid or the basic sites, which agrees with the present results. It is also important

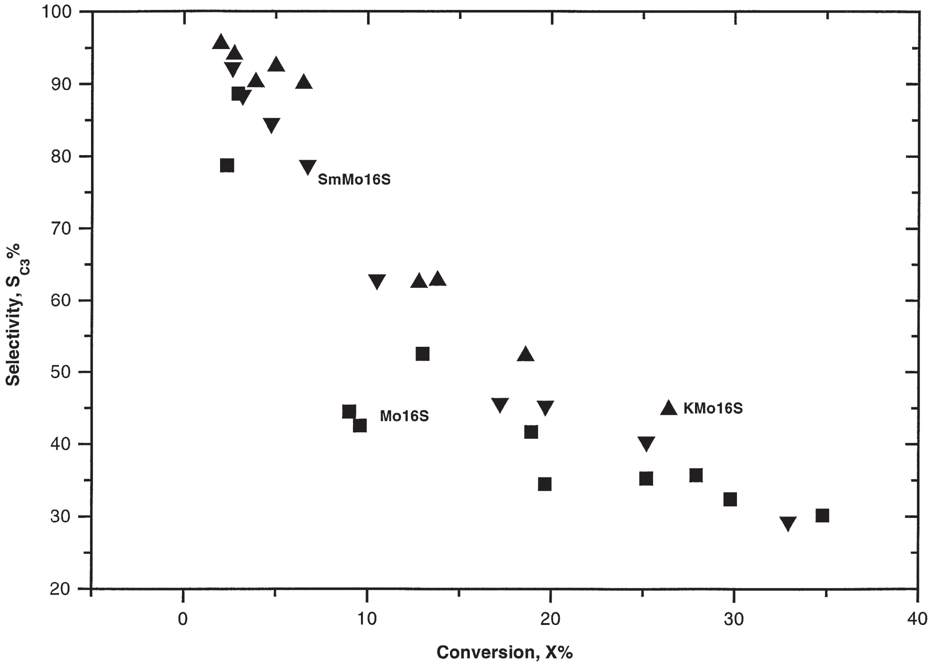

Figure 6. Variation of the selectivity to propene with the conversion of propane.

Table 6
Selectivity to propene at 10 and 20% of conversion on Mo16S and on the modified samples.

| | Mo16S | SmMo16S | KMo16S |
|---|---|---|---|
| $S_{C_3}$ (%) ($X = 10\%$) | 53 | 65 | 78 |
| $S_{C_3}$ (%) ($X = 20\%$) | 35 | 45 | 52 |

to point out that the difference between K and Sm can be due both to the different nature of the promoter and/or to the decreasing promoter concentration as its atomic weight increases.

The addition of K and Sm does not only alter the acidic feature of the Mo16S surface, but significantly affects its redox properties. In spite of the fact that no important changes can be observed in reducibility by TPR measurements, redox changes become obvious from the EPR spectra.

As regards the TPR experiments, only one reduction peak is observed on all samples, which can be attributed to molybdenum species reduced in one step, i.e., $Mo^{6+} \rightarrow Mo^{4+}$. In fact, $MoO_2$ is detected by XRD in all samples after these experiments. The extent of reduction characterized by the amount of hydrogen consumed during the TPR experiments is almost the same on unpromoted and on K-promoted catalysts, whereas it is slightly increased on SmMo16S. This increase could be indicative of some modification in the nature of molybdenum species.

Nevertheless, significant effects on redox properties are found from EPR measurements. The EPR signal for $Mo^{5+}$ is detected in all fresh samples as a consequence of the high calcination temperature [20], being more intense in Mo16S catalyst. The low intensity of the signal on KMo16S indicates a protector effect of the alkaline promoter, which prevents the formation of reduced species during calcination. To a less extent, a similar effect is found on SmMo16S. In any case, significative changes are found in the environmental symmetry of $Mo^{5+}$ ions. The decrease in intensity in the promoted catalysts could be attributed to the formation of new phases which do not alter the $Mo^{5+}$ arrangement. No direct evidence of the formation of these compounds is found. The suppression of the reducibility of $Mo^{6+}$ species could be due to the formation of $K_2MoO_4$ on the surface, as it has been suggested by O'Young [23]. Samarium molybdate could also be formed, but a higher calcination temperature would be needed.

Important changes in line intensity are also found after being used in reaction. Since the EPR technique is a bulk technique, the intensities of $Mo^{5+}$ cannot be used to describe changes on the catalyst surface. However, these changes are observed after being used in the reaction. Thus, it can be inferred that an increase in $Mo^{5+}$ surface concentration is found in all samples, Mo16S being the most intense. Besides, since the incorporation of promoters changes surface architecture, they could modify the spillover species mobility. Ozkan et al. [24] reported that $MnMoO_4$ phase can chemisorb gas-phase oxygen allowing it to migrate, possibly in an activated form, to the reduced site on $MoO_3$ in order to regenerate them.

## *Catalytic activity*

The data mentioned above indicate that modifications of surface acidity/basicity and reducibility of the catalyst lead to different activity/selectivity performance.

Since the ODH reaction involves redox sites [9,13], the catalytic activity must be related to the reducibility of $Mo^{6+}$ species. The intensities of the $Mo^{5+}$ signal decrease in the order Mo16S $>$ SmMo16S $>$ KMo16S. The activity of the catalysts also decreases in the same order. Thus, a parallelism between the concentration of $Mo^{5+}$ species and the catalytic activity can be proposed.

The drawback of potassium addition is a decrease in the catalytic activity, which is in agreement with literature [14,16]. This could be explained by the solid-state reaction consequence of the preparation method. As it has already been mentioned, K can react with $MoO_3$ to form a new phase, such as potassium molybdate, by decreasing the active site concentration for the reaction and the catalytic activity as well. Yoon et al. suggested that the acidic properties on the surface of magnesium molybdate catalysts are responsible for the activities in the ODH of propane [10]. Presumably, the surface molybdenum species cause some acidic sites and activate adsorbed propane. Since the addition of potassium and samarium diminishes the acidic properties, the activity will be lower. Not only is the acidity responsible of decreasing activity but also of stabilizing $Mo^{6+}$, which could not act as readily as a redox-type centre.

The selectivity to propene follows the order of KMo16S $>$ SmMo16S $>$ Mo16S, whereas the strength of acid sites increase in the sequence KMo16S $>$ SmMo16S $>$ Mo16S. Then, it is reasonable to think that the distribution of reaction products depends on the acid character of the catalysts. Olefins interact more strongly with acid catalysts than with basic ones [25]. The desorption of propene intermediate will be faster if a weaker interaction with the surface occurs, thus preventing its further oxidation on the surface to $CO_x$. By comparing the acid character of the catalyst and the selectivity to propene, it can be concluded that the higher the strength and the number of the acid sites on the surface, the lower the selectivity to alkene. This behavior was also found during the ODH of $n$-butane [13].

## 5. Conclusions

The addition of K and Sm to molybdenum supported on $MgO/\gamma$-$Al_2O_3$ catalyst modifies its catalytic performance in the oxidative dehydrogenation of propane. The modifications observed in the redox and acid–base properties of the promoted catalysts explain the different behavior found.

The addition of Sm does not change the whole acidity, but promotes a slight redistribution of acid sites, whereas the addition of K markedly decreases moderate acidity and it correspondingly increases weak acidity.

A protector effect of the promoter which prevents the formation of $Mo^{5+}$ reduced species is found on fresh samples, which is very important on KMo16S. In any case, significative changes are found in the environmental symmetry of $Mo^{5+}$ ions. The addition of promoters changes the surface architecture. They could modify the spillover species mobility affecting reducibility during reaction.

The total activity decreases in the sequence Mo16S $>$ SmMo16S $>$ KMo16S. The selectivities to propene at propane isoconversion increase in the same order. The higher the strength and the number of the acid sites on the surface, the lower the selectivity to alkene. Since $Mo^{5+}$ ions are acid sites, any modification in the redox properties will induce changes in the acid–base properties. A good mixture between acid–base and redox properties seems to be the key in the selective oxidation of propane.

## Acknowledgement

Financial support is acknowledged to CONICET and to Universidad Nacional de San Luis.

## References

[1] M.A. Chaar, D. Patel and H.H. Kung, J. Catal. 109 (1988) 463.

[2] M.A. Chaar, D. Patel, M.C. Kung and H.H. Kung, J. Catal. 105 (1987) 483.

[3] X. Gao, P. Ruiz, Q. Xin, X. Guo and B. Delmon, J. Catal. 148 (1994) 56.

[4] D. Siew Hew Sam, V. Soenen and J.C. Volta, J. Catal. 123 (1990) 417.

[5] S.R. Carrazán, C. Peres, J.P. Bernard, M. Ruwet, P. Ruiz and B. Delmon, J. Catal. 158 (1996) 452.

[6] E. Mamedov and V. Cortes Corberán, Appl. Catal. A 127 (1995) 1.

[7] L.E. Cadus, M.C. Abello, M.F. Gomez and J.B. Rivarola, I&EC Res. 35 (1996) 14.

[8] L.E. Cadus, M.F. Gomez and M.C. Abello, Catal. Lett. 43 (1997) 229.

[9] M.C. Abello, M.F. Gomez and L.E. Cadus, I&EC Res. 35 (1996) 2137.

[10] D. Stern and R. Grasselli, J. Catal. 167 (1997) 550.

[11] Y.S. Yoon, W. Ueda and Y. Moro-oka, Catal. Lett. 35 (1995) 57.

[12] J.C. Vedrine, J.M.M. Millet and J.C. Volta, Catal. Today 32 (1996) 115.

[13] P. Concepción, A. Galli, J.M. Lopez Nieto, A. Dejoz and M.I. Vazquez, Topics Catal. 3 (1996) 451.

[14] A. Galli, J.M. Lopez Nieto, A. Dejoz and M.I. Vazquez, Catal. Lett. 34 (1995) 51.

[15] R.X. Valenzuela, E.A. Mamedov and V. Cortes Corberán, React. Kinet. Catal. Lett. 55 (1995) 213.

[16] R. Grabowski, B. Grzybowska, K. Samson, J. Sloczynski, J. Stoch and K. Wcislo, Appl. Catal. A 125 (1995) 129.

[17] R.M. Martin-Aranda, M.F. Portela, L.M. Madeira, F. Freire and M. Oliveira, Appl. Catal. A 127 (1995) 201.

[18] A. Gervasini and A. Auroux, J. Catal. 131 (1991) 190.

[19] M.F. Gomez, L.E. Cadus and M.C. Abello, Solid State Ionics 98 (1997) 245.

[20] W. Oganowski, J. Hanuza, B. Jezowska-Trzebiatowska and J. Wrzyszcz, J. Catal. 39 (1975) 161.

[21] B.M. Reddy, E.P. Reddy and S.T. Srinivas, J. Catal. 136 (1992) 50.

[22] C. Martin, I. Martin, V. Rives and P. Malet, J. Catal. 161 (1996) 87.

[23] C.L. O'Young, J. Phys. Chem. 93 (1989) 2016.

[24] U.S. Ozkan, M.R. Smith and S.A. Driscoll, J. Catal. 134 (1992) 24.

[25] T. Blasco, P. Concepción, J.M. Lopez Nieto and J. Perez Pariente, J. Catal. 152 (1995) 1.